North Atlantic Aircraft Trajectory Optimization

Olga Rodionova, Mohammed Sbihi, Daniel Delahaye, Marcel Mongeau

North Atlantic aircraft trajectory optimization

Olga Rodionova, Mohamed Sbihi, Daniel Delahaye, Marcel Mongeau [*†]

April 22, 2014

Abstract

North Atlantic oceanic airspace accommodates air traffic between North America and Europe. Radar-based surveillance is not applicable in this vast and highly congested airspace. For conflict-free flight progress, the Organized Track System is established in North Atlantic, and flights are prescribed to follow pre-defined oceanic tracks. Rerouting of aircraft from one track to another is very rarely applied because of large separation standards. As a result, aircraft often follow routes that are not optimal in view of their departure and destination points. This leads to an increase in aircraft cruising time and congestion level in continental airspace at input and output. Implementing new technologies and airborne-based control procedures will enable significant decrease in the present separation standards and improvement of the traffic situation in North Atlantic.

The aim of the present study is to show the benefits that can be expected from such a reduction of separation standards. Optimal conflict-free trajectories are constructed for several flight sets based on the new proposed separation standards, with respect to the flight input data and oceanic winds. This paper introduces a mathematical model; it proposes an optimization formulation of the problem; it constructs two test problems based on real air-traffic data, and it presents very encouraging results of simulations for these data.

[*]Manuscript received ; revised

[†]The authors are with ENAC, MAIAA, F-31055 Toulouse, France and with Univ de Toulouse, IMT, F-31400 Toulouse, France (e-mail: {rodionova, sbihi, daniel, mongeau}@recherche.enac.fr

1 Introduction

The *North Atlantic airspace* (NAT) connects two densely populated continents - North America and Europe. NAT is the busiest oceanic airspace in the world. The Air Traffic Control (ATC) in this airspace is performed by *Oceanic Area Control centers* (OACs). For most NAT, radar surveillance is unavailable, and OACs rely significantly upon the high frequency voice *position reports* communicated by each aircraft for position, progress and intent data [1] (ii, 6.6.18, 17.3.2). This means of communication is not very efficient. Poor propagation conditions can interrupt the provision of necessary information. Thus, aircraft separation and flight safety are ensured in the busy NAT airspace by imposing large *separation standards* to aircraft.

As a result of passenger demand, time zone differences and airport noise restrictions, much of the NAT air traffic contributes to two major alternating flows: a *westbound flow* departing from Europe in the morning, and an *eastbound flow* departing from North America in the evening. This leads to the concentration of most of the traffic unidirectionally, with peak traffic crossing the 30°W longitude between 1130 UTC (Coordinated Universal Time, hours and minutes of the Greenwich mean time) and 1900 UTC for westbound flow, and between 0100 UTC and 0800 UTC for eastbound flow.

Due to the large horizontal separation criteria and a limited economical height band (between *flight levels* (FL) FL290 and FL410 inclusive), the airspace is congested at peak hours. In order to provide the best service to the oceanic traffic, a system of parallel tracks referred to as the *Organized Track System* (OTS) is built to accommodate as many flights as possible within the major flows on, or close to, their minimum-time trajectories and preferred altitude profiles (Fig. 1).

The OTS is constructed twice daily after determination of minimum-time tracks depending on the position of anticyclones and on the dominating winds. OAC planners rely on the airline preferred routes and altitude profiles, also taking into account the requirements from adjacent OACs and domestic ATC agencies, the opposite direction traffic, the airspace restrictions (danger area, military airspace reservations, etc.) [1] (2.2.1, 17.3.4). Due to the energetic nature of the NAT weather patterns, including the presence of jet streams, consecutive eastbound and westbound minimum-time tracks are seldom identical. The creation of a different OTS is therefore necessary for each of the major flows. In general, the eastbound (night-time) tracks (produced by Gander OAC) are located more northerly than the westbound

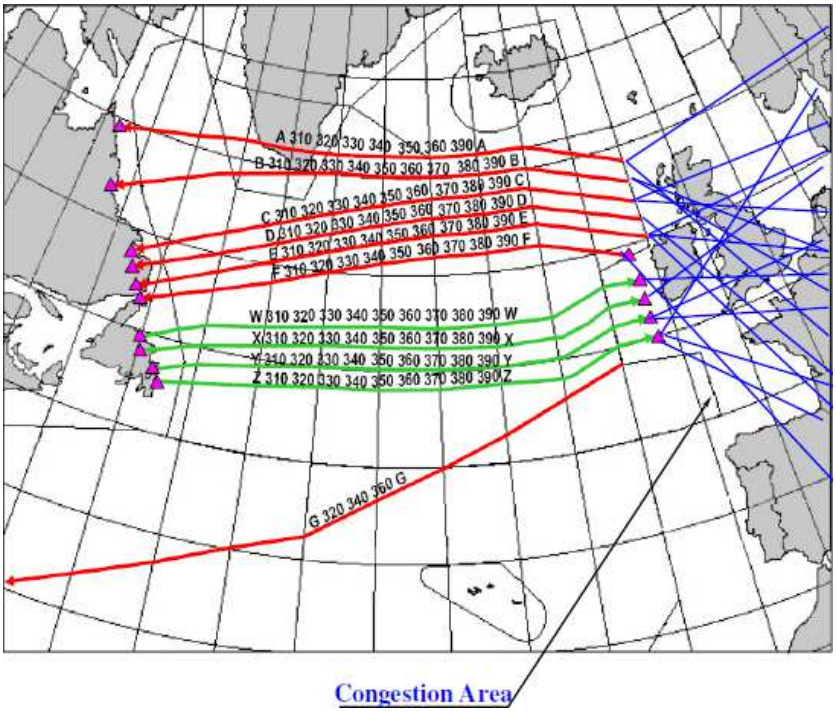

Figure 1: The Organized Track System

(day-time) tracks (produced by Shanwick OAC) (Fig. 1).

Currently, about half of NAT flights utilize the OTS [1] (2.1.3). All OTS flights operate on great circles joining successive significant *waypoints* (WPs); and are commonly planned so that the specified ten degrees of longitudes (10°W, 20°W etc.) are crossed at integer degrees of latitude [1] (4.1.2). The OTS WPs include *named* significant points and latitude crossings of all oceanic ten-degree meridians. The OTS is constructed so that the *lateral separation* of 60 NM (111.11 km) is automatically maintained for aircraft on adjacent tracks. Most adjacent tracks are separated by 1° of latitude at each WP.

Vertical separation is ensured through the use of predefined FLs. The distance between adjacent FLs is 1000 feet (304.8 m). The aircraft intending to follow an OTS track may be planned at any of the FLs published for that track on the current daily NAT message. Step climbs may also be included in the *flight plan* (FPL), although each change of FL during flight must be requested from ATC.

Longitudinal separations between subsequent aircraft following the same track (*in-trail*) in the NAT airspace are assessed in terms of differences in actual and estimated times of arrival at common waypoints; and expressed in clock minutes. On applying the time-based separation minimum, one must take care that this minimum is not to be violated whenever en route (including the case when the following aircraft maintains higher speed than the preceding one). When aircraft are expected to reach minimum separation, speed control is to be applied [2, (5.4.2)] .

The maintenance of in-trail separation is aided by the application of the *Mach number technique*, i.e. a technique whereby aircraft operating successively along suitable routes are cleared by ATC to maintain appropriate *Mach numbers* for a portion of the en-route phase of their flight [1] (7.1.1). Practical experience has shown that when the aircraft operating along the same route at the same FL maintain the same Mach number, they are more likely to maintain a constant time interval between each other. This is due to the fact that the aircraft concerned are normally subjected to approximately the same meteorological conditions, and minor variations in ground speed tend to be neutralized over long periods of flight.

According to the *current separation standards* (CSS) in NAT [1] (9.1.4), two consecutive aircraft following the same track should be separated at least 10 minutes apart (Fig. 2). (This norm can be reduced up to 5 minutes if the preceding aircraft is faster than the following one [2, (5.4.2)]; we neglect this fact in our model, which is therefore likely to produce suboptimal but acceptable solutions from the operation point of view as it is subjected to stricter constraints). Their longitudinal relationship is established by their position reports, and any errors in forward position estimates can be assumed to cancel out, since they both experience the same weather. In the case where it is desired to move a particular aircraft onto the adjacent track, this cancelling-out of weather errors cannot be assumed to have occurred because of the difference in meteorological conditions between the tracks. As a consequence, current regulations impose an increased longitudinal separation of 15 minutes in this case [3] (Fig. 2).

The current situation for oceanic traffic on the OTS shows that aircraft often follow routes which are not optimal in terms of flow management from an overall ATC point of view [3], and therefore re-routing is necessary when entering continental radar control area. This leads to increasing length and duration of the flights as well as to increasing the congestion in the continental airspace near the exit of the OTS (Fig. 1).

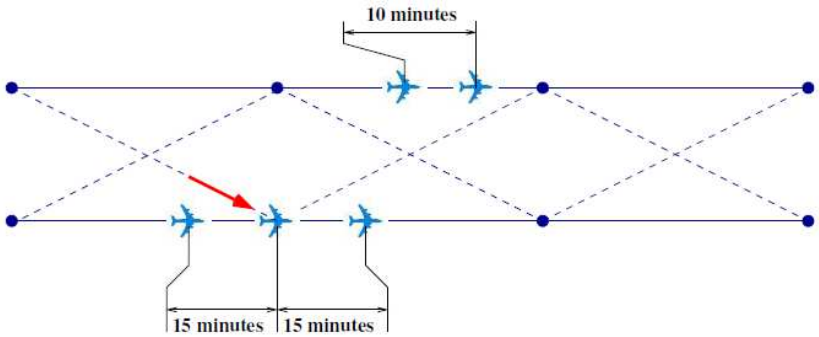

Figure 2: Longitudinal separation standards

It seems reasonable to enable re-routing of aircraft from its initial track to another oceanic exit point, more suitable regarding its final destination, directly within the OTS covered area. This would reduce congestion in continental airspace near OTS exit and improve the aircraft remaining route towards destination. A major factor in preventing traffic re-routing with CSS is the additional longitudinal separation required for flights which have not reported over a common point. Due to the high density of traffic on tracks and the need for large longitudinal separations, this re-routing maneuver can rarely be applied on the OTS [3].

The transition from present ATC tools to airborne-based systems and procedures proposed by American and European projects NextGen (Next Generation Air Transport System) and SESAR (Single European Sky ATM Research) can help overcome these drawbacks. Thanks to new technologies (such as the *Automatic Dependent Surveillance-Broadcast* technology [4]), the airborne delegated separation can be applied to aircraft [5]. The new approach will allow significant decrease in the oceanic separation standards [6], i.e. consecutive aircraft following the same track would be separated by only around 2 minutes [3], and an aircraft performing a re-routing to the adjacent track would be separated by around 3 minutes from aircraft on this track. Obviously, such *reduced separation standards* (RSS) will increase the maximum number of aircraft on tracks as well as the number of possible flight re-routes [7]. In consequence, this will raise the limit on the total number of flights in the NAT airspace, and generally improve the aircraft routes by decreasing their length.

Several papers [8, 9, 10, 11] are devoted to related problems in the Pa-

cific oceanic airspace. However, to our knowledge, no research work has been published concerning the NAT airspace. Preliminary results obtained from modelling the oceanic air traffic situation in NAT when reducing the separation standards are described in [12].

This paper presents a mathematical model for the described problem and its application to real oceanic air-traffic data. The aim of this study is to provide the correct FPLs for NAT flights satisfying the flight restrictions (departure and destination points, speed, FL, etc.), taking into account the RSS. Section 1 describes the mathematical formulation of the problem. Section 2 presents the optimization algorithm developed to solve the problem. In Section 3, the studied air traffic data is described, and in Section 4, the simulations for this data are performed and the results are analyzed.

2 Mathematical formulation of the problem

In this section, we propose a mathematical formulation of the problem consisting in searching for the optimal FPLs for a set of flights within OTS. As the subject of the study is the NAT airspace, only the parts of the routes belonging to the OTS are taken into account. Moreover, as eastbound and westbound traffic are separated in time (due to the specific demands) and in space (correspondingly with the OTS structure), they can be considered independently. Thus, without loss of generality, in this study only the eastbound traffic (cruising from North America to Europe) is taken into consideration.

2.1 OTS model and flight model

The OTS is represented by an $Nx \times Ny \times Nz$ grid of WPs, where Ny is the number of OTS tracks, Nx is the number of WPs on each track, and Nz is the number of FLs for each track. The tracks are labelled from 1 to Ny starting from the most northern, the WPs on each track from 1 to Nx starting from the most western, and the FLs from 1 to Nz starting from the lowest. Thus, the 3D position of an aircraft on track j at WP i at FL k is completely specified by the vector (i, j, k).

A flight entering a predefined track at a predefined FL is supposed to follow this track at the same FL until any change of the trajectory is made. In this study, such changes are only allowed at the WPs. Thus, from the current WP (i, j, k), the flight has several possibilities to pursue its route:

- follow the same track at the same FL

- re-route to an adjacent track at the same FL

- change the FL

In the first two cases, the flight will follow the straight line connecting the current WP with the next one, where the next WP can be one of the following (Fig. 3):

- $(i+1, j, k)$ (same track)

- $(i+1, j-1, k)$ (northern re-route)

- $(i+1, j+1, k)$ (southern re-route)

These straight lines (route segments) are called *links*. Each WP (except for those on the outer tracks) has three outgoing links. The link intersection points are called *nodes*. The *nodes* are of two types: the *WPs*, that are located on tracks and belong to the OTS grid structure, and *extra nodes*, that are placed at the points of intersection of the links, joining the adjacent tracks, i.e. the links of the form (i, j, k)-$(i+1, j+1, k)$ and $(i, j+1, k)$-$(i+1, j, k)$.

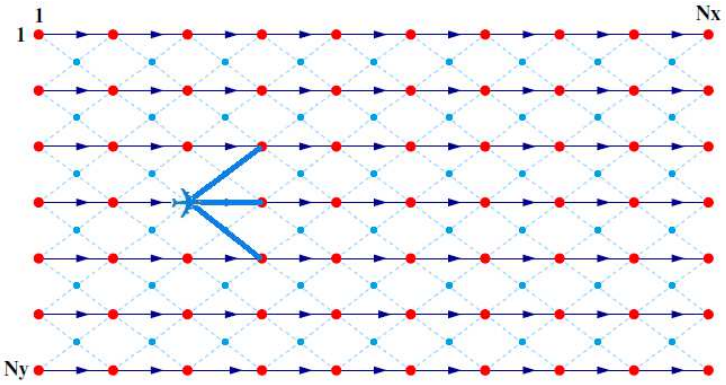

Figure 3: OTS grid model with nodes and links in horizontal dimension

When changing its FL, an aircraft is only authorized to climb, in order to satisfy the optimal kerosene consumption flight profile provided by the airline company. Moreover, according to the current ATC rules [1], aircraft

may change FL only at WPs (Fig. 4). In our model, the distance between the real horizontal position of the aircraft at the new FL and the previous WP (see Fig. 4) is neglected, as well as the time required to reach the new FL. This instantaneous-climbing hypothesis is reasonable, as the distance between the WPs (10° of longitude, that is about 500 km) is much longer than the distance between FLs (1000 feet, equal to 0.3048 km).

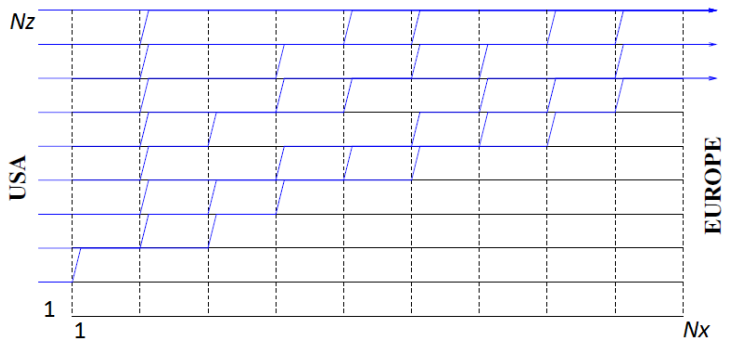

Figure 4: Flight-level change model on a given track. Section of OTS in vertical dimension

Each flight is modelled by few parameter values, some of which are fixed data of the problem, while the others can be modified and represent the model optimization variables, i.e.:

- entry and exit tracks
- track entry time
- speed and FLs at the WPs
- track change positions

The number of possible options given to a flight depends on its entry and exit tracks. For instance, if the entry and exit tracks are the same, we suppose in this study that the aircraft has no opportunity to vary its trajectory. The FL and speed changes are fixed according to the optimal aircraft performance and happen at some pre-computed WPs. They are not decision variables.

2.2 Optimization model

In this work, a simplified model is considered. For each flight f, the following **input data** are given:

- $TD^f_{in} \in \{1, 2, \cdots, Ny\}$ - the desired entry track
- $TD^f_{out} \in \{1, 2, \cdots, Ny\}$ - the desired exit track
- $t^f_{in} \in I\!R^+$ - the desired entry time
- v^f_i, $i = 1, 2, \cdots, Nx$ - aircraft speeds at WPs preserved along outgoing links
- $FL^f_i \in \{1, 2, \cdots, Nz\}$, $i = 1, 2, \cdots, Nx$ - flight levels at WPs defining the flight altitude profile and satisfying the following conditions: $FL^f_{i+1} \geq FL^f_i$, $i = 1, 2, \cdots, Nx - 1$.

For each flight f, the **decision variables** are defined as follows:

- x^f_i, $i = 1, 2, \cdots, Nx - 1$ - binary variables defining the flight re-routing maneuvers:
  $x^f_i = \begin{cases} 1 & \text{if flight } f \text{ changes track at WP } i, \\ 0 & \text{otherwise.} \end{cases}$

For each flight f, x^f_i form a binary vector of size $Nx - 1$, where the number of ones is equal to the distance between the entry and exit tracks. When $x^f_i = 1$, the aircraft leaves its current track at WP i, and reroutes to the appropriate adjacent track: the next track towards the exit track (assuming that an optimal trajectory will not involve north-south zigzaggings).

Preliminary experiments have shown that for many practical cases, this state space definition is not rich enough to guarantee conflict-free trajectories. To avoid this situation, entry and exit track numbers and entry time have been relaxed. Thus, an aircraft is allowed to enter/exit an adjacent track. Moreover, this can be done with some entry delay denoted by d^f, that is chosen among a number, N_d, of discrete values multiple of a fixed time duration denoted as *slot*. More precisely, the new associated **decision variables** for flight f are:

- $TA^f_{in} \in \{1, 2, \cdots, Ny\}$ - the assigned entry track

- $TA^f_{out} \in \{1, 2, \cdots, Ny\}$ - the assigned exit track
- d^f - the time delay at track entry

These decision variables must satisfy the following **constraints** for each flight f:

- $TA^f_{in} \in \{TD^f_{in} - 1, TD^f_{in}, TD^f_{in} + 1\}$, (tolerance with regards to the desired entry track)
- $TA^f_{out} \in \{TD^f_{out} - 1, TD^f_{out}, TD^f_{out} + 1\}$, (tolerance with regards to the desired exit track)
- $d^f = \delta^f \cdot slot$, where $\delta^f \in \{0, 1, ..., N_d\}$, $slot \in \mathbb{R}^+$ (acceptable entry delays)
- $\sum_{i=1}^{Nx-1} x_i^f = \left| TA^f_{out} - TA^f_{in} \right|$, (total number of re-routing maneuvers)

In addition to this, the decision variables should provide a conflict-free solution. Based on the route network structure (Fig. 3), conflicts may happen only at nodes and links. The following auxiliary optimization variables are introduced:

- C_n - the total number of conflicts on nodes
- C_l - the total number of conflicts on links
- $C_t = C_n + C_l$ - the total number of conflicts

Thus, the last **constraint** included in the formulation of the optimization problem requires the absence of conflicts:

- $C_t = 0$ (collision-avoidance)

Given an instantiation of the decision variables, the aircraft trajectories can be computed on the OTS grid using a flight simulator. Each time an aircraft f passes over a node n, the passing time t^f_n is recorded. The same recording process is applied for link entry and exit times.

A conflict is detected on a node if the longitudinal separation constraint is violated for two aircraft passing this node. For a given node n, all the flights

f passing this node (N_n flights) are selected and sorted according to their times t_n^f. To satisfy the longitudinal separation requirements, the condition $t_n^{f_{i+1}} - t_n^{f_i} \geq \Delta t_s(f_i, f_{i+1})$ must be fulfilled for $i = 1, 2, \cdots, N_n - 1$, where $\Delta t_s(f_i, f_{i+1})$ is the longitudinal separation value depending on the separation standards (CSS or RSS) and on the flight maneuvers (moving straight, re-routing or climbing, see Fig. 2). If for any consecutive flights f_i and f_{i+1} this condition is violated, then a conflict is detected and C_n is increased by one.

A conflict can happen on a link if one aircraft is slower than the other following it on the same track. Link conflicts can be detected based on the aircraft sequence order at the link entry and exit. All flights passing a particular link l are selected and sorted into two lists according to the times at which they enter and exit this link. Then, the entry and exit lists are compared. If two aircraft are found to be swapped, then a conflict is detected and C_l is increased by the number of flights having different ranks in both lists.

For a set of flights, different route optimality criteria exist, e.g. trajectory length, flight duration, fuel consumption, etc. In this paper, we consider including the following criteria related with aircraft route in the objective function:

- D - the total entry delay
- P - the total cruising time within the OTS
- G - the total deviation delay

The total entry delay, D, is obtained by summing up the track-entry delays d^f over all flights f: $D = \sum_{f=1}^{N} d^f$. The total cruising time P is the sum of the cruising time of each single aircraft p^f, i.e. the time between aircraft entering and exiting corresponding OTS tracks, over all aircraft: $P = \sum_{f=1}^{N} p^f$. The cruising time is directly related to fuel consumption; that is the major criterion for airlines.

The total deviation delay, G, sums up (over all flights) the time necessary for each aircraft to reach its desired entry/exit track from its assigned entry/exit track. Let S_{in}^f denote the distance between TD_{in}^f and TA_{in}^f (the distance between the corresponding entry WPs) for flight f , and let S_{out}^f be the distance between TD_{out}^f and TA_{out}^f. Recall that the aircraft speeds at entry and exit WPs are denoted as v_1^f and v_{Nx}^f respectively. Then, G is calculated as follows: $G = \sum_{f=1}^{N} [S_{in}^f / v_1^f + S_{out}^f / v_{Nx}^f]$. Remark that G is an

artificial measure, introduced to penalize solutions involving flights deviated from their desired entry/exit tracks, (i.e. when a flight is assigned an adjacent track instead of its desired track). As a result, G involves coherent units of measurements.

All the presented values are expressed in terms of time and are to be minimized. Thus, they can be accumulated in a single objective function using appropriate (non-negative) weighting coefficients (α, β, γ) set by the user according to his priorities, enabling inclusion/exclusion of different criteria in the objective function, trade-offs, etc.:

- $F_{obj} = \alpha D + \beta G + \gamma P$.

Results from the preliminary study [12] show that a conflict-free solution may not exist in some practical cases, so, the collision-avoidance constraint cannot be satisfied. Furthermore, even in cases where conflict-free trajectories do exist for a given set of flights, finding such an acceptable configuration is not an easy task. In order to overcome this difficulty, we propose to allow the violation of the collision-avoidance constraint. To do so, we include a collision-avoidance constraint violation measure, the total number of conflicts C_t, as an additional criterion in the objective function, using an additional non-negative weighting coefficient, ϕ:

- $F_{obj} = C_t + \phi(\alpha D + \beta G + \gamma P)$.

Minimizing such an objective function will enable the elimination of conflicts while reducing en-route delays. The choice of a small value of ϕ yields the highest priority to the conflict-free criterion, when solving the problem. Once all the conflicts are eliminated (if it is possible), the en-route delays are reduced, while ensuring that the considered solutions remain conflict-free.

2.3 Possible model extensions

As mentioned above, a simplified model is considered in this preliminary study. This section gives some remarks on how the model can be extended to include more options and criteria to approach the real air-traffic situation in NAT.

- Different criteria (R_k) reflecting the traffic performance (e.g. total flight duration, total fuel consumption) can be included into the objective function with corresponding weighting coefficient (α_k):

$F_{obj} = C_t + \phi(\sum_k \alpha_k R_k)$.

- The weighting coefficients for different criteria in the objective function can be adjusted independently for each flight, to permit the airlines to define the optimization priorities for each particular flight. Considering the coefficients α_k^f that correspond to the criterion R_k having the values r_k^f for flight f, we obtain:
  $F_{obj} = C_t + \phi(\sum_k \sum_{f=1}^{N} \alpha_k r_k^f)$.

- The aircraft speeds (v_i^f) and/or FLs (FL_i^f) at WPs can be considered as decision variables. That would give more flexibility to find feasible solutions, eventually increasing the model complexity. In this case the objective function should include fuel consumption criterion.

- The optimal aircraft speeds and flight altitude profiles can vary depending on the OTS tracks attributed to the flight. The input data of the model can be modified so that to accept track-dependent speeds ($v_{i,j}^f$) and FLs ($FL_{i,j}^f$) for each flight f.

3 Problem resolution via Genetic Algorithm

In this section the algorithm used for solving the described optimization problem is presented. The problem to be solved is fully discrete with numerous decision variables. If we consider N flights with a number of discrete delays N_d and if we suppose that an average number N_c of track changes among $Nx-1$ transition segments are required, the total number of possible combinations of decision variable values would be: $\left((N_d+1) \times \begin{pmatrix} Nx-1 \\ N_c \end{pmatrix}\right)^N$. For instance, if $N = 500$, $N_d = 5$, $N_c = 4$ and $Nx = 10$, then there would be *a priori* 756^{500} possible solutions to be considered.

Due to this high combinatorics, a *Genetic Algorithm* (GA) has been implemented. GA is inspired by the evolution theory concepts such as *mutation*, *crossover* and *selection* [13, 14]. Each possible solution is encoded as an *individual*. The algorithm randomly creates first *population* (set of individuals). Each individual ability to solve the problem (the *fitness*) is then evaluated. The best individuals (according to their fitness) are selected, and then crossovers and mutations are applied to obtain a new population (the next *generation*).

In our context, an individual represents the trajectories of the set of N flights using N vectors, each of which corresponds to a particular flight. The vector associated with flight f contains the decision variables introduced above: $\delta^f, TA^f_{in}, TA^f_{out}, x^f_i, i = 1, 2, \cdots, Nx-1$ (Fig. 5). The flight trajectory is completely defined by these variables together with the flight input data (i.e. the desired track entry time, the flight altitude profile and the aircraft speeds).

Furthermore, the genetic operators are adapted to the problem under study. The mutation operator aims at diversifying the *genes* (features, or components, of a solution) in the population in order to explore as widely as possible the search space. For our problem, a *single mutation* consists in choosing randomly one flight, f, and changing randomly some of its parameters. The single mutation of re-routing variables involves choosing randomly two variables x^f_i and x^f_j having different values (0 and 1), and permuting their values (Fig. 5). Thus, a single mutation is applied to a *single trajectory*.

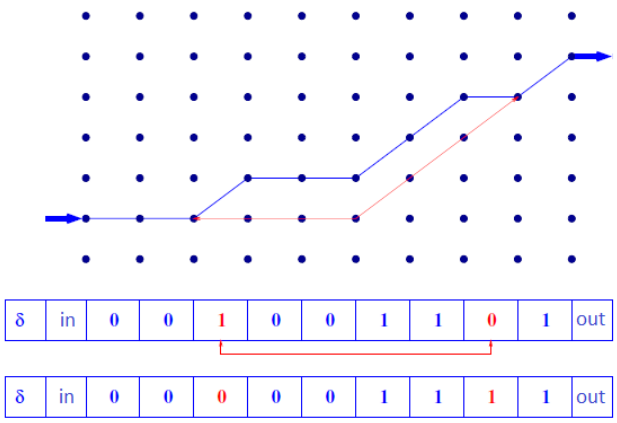

Figure 5: Flight trajectory encoding. Mutation operator applied to a trajectory

The crossover operator aims at finding better solutions by combining features of two good individuals from the previous generation. The chosen crossover operator randomly selects some trajectories of one individual and swaps them with the corresponding trajectories of another individual (Fig. 6). Note that such a crossover operator, swaps the full trajectories (a particular trajectory cannot be cut in the middle to be concatenated with the corresponding part of another trajectory). In other words, it is applied

to the *set of flights*.

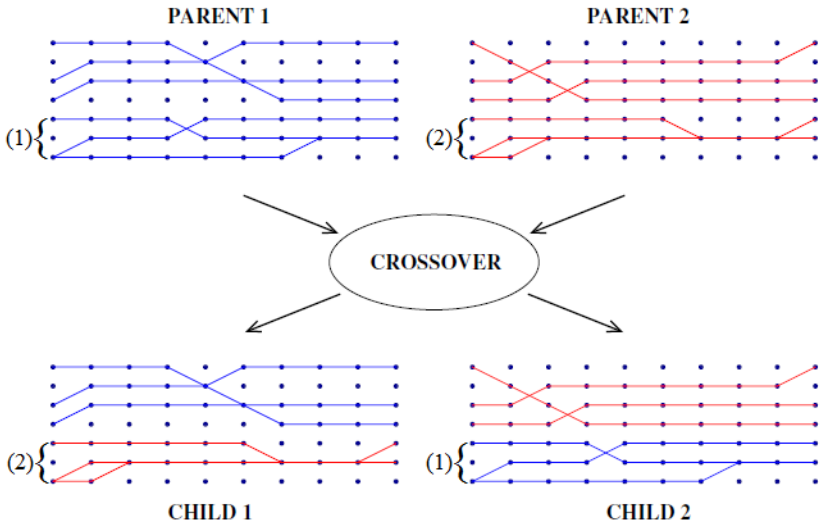

Figure 6: Crossover operator applied to two flight sets

The above-described encoding and the mutation and crossover operators are such that, by construction, they produce feasible solutions (sets of trajectories) satisfying airline preferences (entry/exit points, no zigzagging between tracks) and ATC constraints (re-routing at WPs).

The GA terminates the execution either if the acceptable solution is obtained (for example, if we focus on conflict elimination only, the algorithm stops once $C_t = 0$ for any individual), or if the computational budget is exhausted, i.e. the maximal number of generations, N_G, is achieved (N_G is to be set by the user).

4 Input data for simulations

The developed algorithm was applied to perform the simulations of real oceanic traffic situation in NAT. In this section we present the general features of the air-traffic data used in the test problems, we define the desired entry and exit tracks, we describe the oceanic winds involved, and we make some remarks concerning the initial flight plans.

4.1 Test problems

Two days were selected for simulations: **August 3, 2006** and **August 4, 2006**. The oceanic traffic data was obtained from the report files from Shanwick OAC. Each such file contains the report messages from different sources, including NAT messages, FPL messages, flight position reports, etc.

The OTS was modelled with a grid of WPs extracted from NAT messages. For the two selected days, the OTS consists of $Ny = 6$ tracks (U, V, W, X, Y and Z) having $Nx = 8$ WPs each and $Nz = 9$ FLs (from FL320 to FL400 inclusive). The WPs are defined by their geographic coordinates.

The set of flights for each of the studied days was extracted from FPL messages. We select only the flights that:

- have all information necessary for simulations:
    - departure and arrival airports
    - estimated elapsed times (EETs) at WPs
    - aircraft speed and FL at least at one of the WPs
- are eastbound (cruising from North America to Europe)
- are planned completely on the OTS, i.e.
    - follow a single OTS track from its entry point to exit
    - or perform the re-routing from one track to another but with respect to the WPs sequence
- utilize the night-time OTS during its period of validity
- occupy the FLs in the range declared for this OTS

The flights where FPLs do not satisfy these conditions are not taken into consideration. Thus, for the studied days we obtained the flight sets consisting of:

- $N = 331$ flights, for August 3rd, 2006
- $N = 378$ flights, for August 4th, 2006

For these acceptable flights, the input data is extracted from the FPLs. The track entry time (t_{in}^f), if not defined directly, is calculated using the EETs declared for the following track WPs and the estimated times of cruising between the WPs. Aircraft speeds (v_i^f) and FLs (FL_i^f), if not defined directly at some WPs, are extrapolated from previous WPs.

The resulting files with extracted data used in simulations can be found at [15].

4.2 Definition of desired entry and exit tracks

In this study we consider that the *desired* entry and exit tracks (TD_{in}^f and TD_{out}^f) are those *closest* to the departure and arrival airports (i.e. the desired entry track is the track which entry point is the closest to the departure airport). Such *desired track* definition permits to reduce the continental route crossings and, therefore, to reduce airspace congestion.

Figure 7 compares the entry and exit tracks defined in FPLs with the desired entry and exit. As can be seen from this diagram, according to FPLs, aircraft should generally follow tracks that are not optimal in terms of entry and exit points. Only about 20% of all flights enter the desired track, and only about 17% of flights exit the desired track.

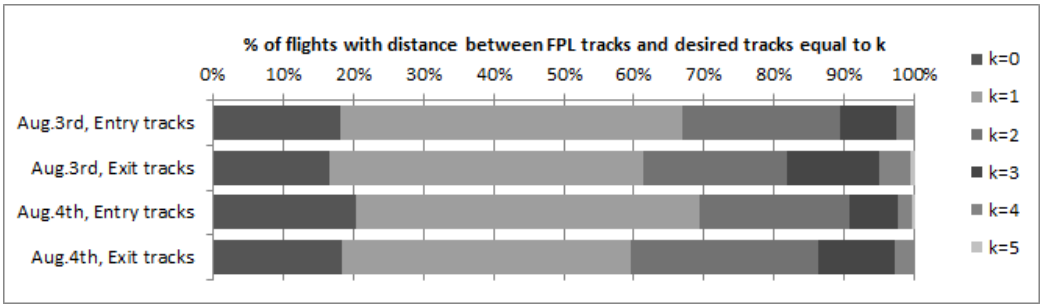

Figure 7: Comparison of FPL declared entry and exit tracks with corresponding computed desired tracks

To show the advantages of using desired entry/exit tracks (based on the airport coordinates) rather than FPL-declared entry/exit tracks, we have calculated the number of flight route crossings in the continental airspace before entering and after exiting NAT. To do so, in each of the continental airspace, we consider the flight route as an arc of the great circle, going from

the departure airport to the track entry point, and from the track exit point to the arrival airport, respectively. The route crossing is considered to be equivalent to the crossing of these arcs, not taking into account departure times. The airspace congestion is evidently related with the number of such route crossings. On the other hand, the flights, utilizing the same routes in continental airspaces, as well as the flights entering/exiting the same tracks also make the contribution to congestion level. These situations are considered to be managed more easily than crossings. The corresponding quantities are p resented in Table 1.

Table 1: Flight route crossings in continental airspace

	FPL	Desired	FPL	Desired
Date	August 3rd		August 4th	
Total NbF (N)	331		378	
For American continental airspace before entering NAT				
Nb departure airports	33		38	
Total NbR	88	33	101	38
Max NbF for track	86	240	104	263
NbR in common	47	20	62	22
NbF with common routes	290	318	339	362
Max NbF for route	23	67	26	74
NbR crossings	961	0	1447	0
NbF crossings	12736	0	17316	0
For European continental airspace after exiting NAT				
Nb arrival airports	44		51	
Total NbR	92	44	97	51
Max NbF for track	88	231	105	267
NbR in common	49	29	53	29
NbF with common routes	288	316	334	356
Max NbF for route	27	57	31	60
NbR crossings	677	0	497	0
NbF crossings	5308	0	4872	0

In Table 1, the columns "FPL" correspond to flight sets with entry/exit tracks extracted from FPLs, while the columns "Desired" give the values for flights with entry/exit tracks closest to departure/arrival airports. The abbreviation "Nb" stands for "Number"; "NbR" means "Number of routes"

(here the routes in continental airspaces are concerned); and "NbF" means "Number of flights". One can notice, that even if the number of common routes (NbR in common) is almost twice as low for the "Desired" approach, the number of flights utilizing these routes (NbF with common routes) is greater in this case. Moreover, there are more aircraft on a single route, as well as much more aircraft entering/exiting a single track for the "Desired" approach. This can augment the continental congestion. On the other hand, Table 1 presents two quantities for crossings: the *number of route crossings* (NbR crossings) not taking into account the number of aircraft using these routes, and the *number of flight crossings* (NbF crossings), which depends on the number of aircraft using crossing routes. According to the initial FPL, crossings are quite numerous. However, for the "Desired" approach, there are no route crossings in the continental airspace, as expected. This choice would therefore decrease the congestion level.

4.3 Definition of wind speeds

During the simulations, wind is taken into account. The average tail wind speeds between the OTS WPs were calculated on the basis of the estimated times of cruising between these WPs, obtained from ETAF (Elapsed Time And Forecast) messages. When performing the flight progress, the aircraft ground speed is computed by adding the corresponding wind speed to the aircraft speed declared in the FPL.

Figure 8 represents the distribution of the wind between the OTS tracks on August 3rd for the most occupied flight level, FL370. Each column of the diagram represents the average tail wind speed between the corresponding WPs (in m/s). One can observe that the wind significantly differs from one track to another. At the west part of the OTS it is more preferable to use southern tracks, while for the east part the northern tracks feature stronger winds (what corresponds to the way of OTS construction). For August 4th, the wind distribution is almost the same.

4.4 Evaluation of initial FPLs via the number of conflicts en route

In this section we present some remarks concerning initial FPLs extracted from the record files. Each flight trajectory is defined in the FPL via the

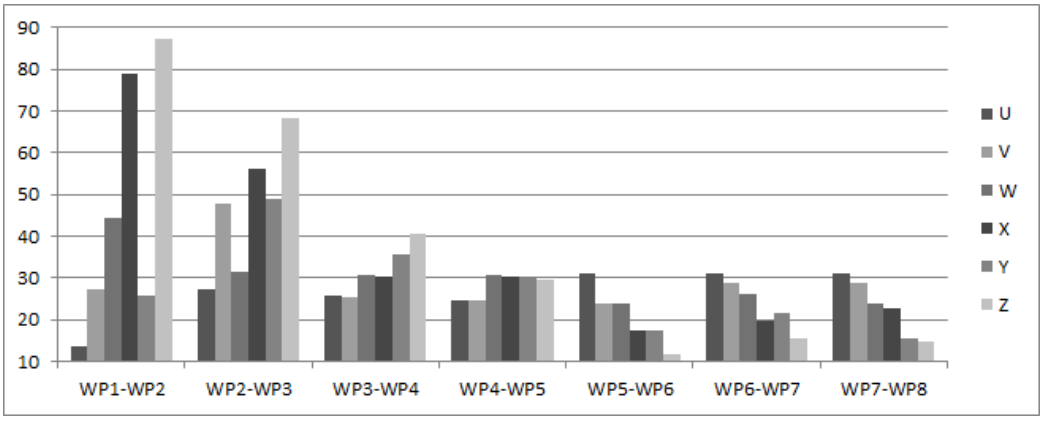

Figure 8: Wind speeds (m/s) between track waypoints on FL370 for August 3rd, 2006

sequence of WPs followed in some cases with particular FLs and/or Mach numbers. We express this trajectory data in terms of the mathematical model parameters: TD^f_{in}, TD^f_{out}, t^f_{in}, v^f_i, FL^f_i and x^f_i. Furthermore, we consider: $TA^f_{in} = TD^f_{in}$, $TA^f_{out} = TD^f_{out}$, and $d^f = 0$, for each flight f. W obtain thereby one instantiation of the optimization problem. Further, this set of trajectories is evaluated over the corresponding OTS grid and the number of conflicts, C_t, induced by these flights is computed. As one can see from the results of this simulation presented in Table 2, even with RSS, there still remain aircraft in conflict according to their initial flight plans. Thus, the published FPLs for the two sets of flights could not be fulfilled in reality.

Table 2: Conflicts produced by sets of flights declared in FPL messages

Date	August 3rd	August 4th
Total number of flights (N)	331	378
Number of conflicts, C_t, CSS	811	876
Number of conflicts, C_t, RSS	245	259

Table 3 reveals how the flights in the reality are deviated from their initial FPLs. For each of the days, the percentage of flights having different route parameters (tracks, FPLs, speeds, entry times) than those defined in the FPL, is presented. Remark that almost all flights are affected by deviations.

The goal of the simulations presented in Section V is to produce new FPLs for the sets of flights with respect to the desired departure and arrival

Table 3: Percentage of aircraft having en-route flight parameters different from those defined in initial FPL

% of flights with different:	August 3rd	August 4th
Routes (Tracks/WPs)	2,4%	3,4%
Flight levels	40,8%	45,5%
Speeds	23,3%	26,5%
Track entry time	96,7%	97,1%
Track entry time > 30 minutes	65,6%	67,5%
Track entry time > 2 hours	8,8%	19,3%

points and track entry time that would guarantee no conflicts, at least with RSS.

5 Computational results

This section presents some results obtained with the GA applied to our optimization problem on the real oceanic traffic data. The aim of these simulations is to find better trajectories for the given sets of flights and to show the benefits expected from the decrease of the separation standards as a result of the use of new technologies.

The GA was implemented in Java and run under Windows-32 operating system, on Intel Core i7-3610QM CPU with 2.30 GHz.

Two types of tests were held for each of the studied flight sets (August 3rd, 2006 and August 4th, 2006): with CSS and with RSS (considering all aircraft to possess the appropriate equipment).

The aircraft were allowed to select an entry time delay multiple to $slot$=5 min (0, 5, 10, etc. minutes). Various maximum values of acceptable delays, N_d, were tested. Note that in reality the entry time delay is assigned to the aircraft at the departure airport before take-off (not before entering the track in the air); thus, important delays are still acceptable.

5.1 Simulations with current separation standards

When applying the CSS, we concentrate on eliminating en-route conflicts:

- $F_{obj}^{(1)} = C_t$

In these simulations, the value of the separation criterion, $\Delta t_s(f_i, f_{i+1})$, is 10 minutes for consecutive aircraft and 15 minutes for re-routing aircraft. The number of acceptable delays, N_d, was set to 6; thus, the maximum value of track entry delay, d, is 30 minutes. Several tests were performed with different numbers of generations: $N_G = 1000, 3000, 5000$. The results of simulations with $N_G = 3000$ for both studied flight sets are presented in Table 4.

Table 4: Results of GA application to real oceanic traffic with CSS

Test	Number of flights	Number of conflicts, C_t		CPU time (min.)
		initial	best	
August 3rd	331	1103	121	13,5
August 4th	378	1367	219	15,5

These results show that the GA could not find conflict-free solutions for the flight sets with CSS, neither for August 3rd nor for August 4th. This fact tends to confirm that, with CSS, the aircraft cannot fly optimal routes, resulting in augmenting the cruising time and in increasing congestion in continental airspace. This motivates the reduction of separation standards.

5.2 Simulations with reduced separation standards

The major subject of this study is oceanic air traffic with RSS. In the first stage, the optimization aims at obtaining conflict-free trajectories for such standards:

- $F_{obj}^{(1)} = C_t$

Furthermore, we also intend to observe the effect of including other criteria in the objective function. In this section, we choose the total entry delay, D, and the total deviation delay, G, to be minimized. The weighting coefficients are set to: $\alpha = 1$, $\beta = 1$, $\gamma = 0$.

- $F_{obj}^{(2)} = C_t + \phi(D + G)$

In these simulations the value of the separation criterion, $\Delta t_s(f_i, f_{i+1})$, is 2 minutes for consecutive aircraft and 3 minutes for re-routing aircraft. The number of generations, N_G, is set to 1000 (this value was empirically observed sufficient to obtain conflict-free solutions). The tests are performed

Table 5: Results of GA application to real oceanic traffic with RSS

F_{obj}	N_d	CPU time (min.)	% of flights with TD^f_{in}	% of flights with TD^f_{out}	% of flights with $d^f = 0$	D_t (hours)
August 3rd, 331 flights						
$F^{(1)}_{obj}$	6	0,5	93,4%	93,6%	14,5%	83,2
$F^{(1)}_{obj}$	1	1	89,4%	88,5%	48,9%	14,1
$F^{(2)}_{obj}$	1	4,5	93,7%	93,4%	74,0%	7,2
August 4th, 378 flights						
$F^{(1)}_{obj}$	6	1	92,3%	92,1%	14,0%	95,9
$F^{(1)}_{obj}$	1	4,5	85,7%	81,5%	53,7%	14,6
$F^{(2)}_{obj}$	1	5	92,9%	92,1%	73,5%	8,3

with different values of acceptable delays, N_d. Some results of simulations (for $N_d = 6$ and $N_d = 1$) are presented in Table 5.

The first important conclusion is that, with RSS, conflict-free configurations of trajectories do exist for all studied flight sets. This shows that implementing new technologies can yield a strong positive effect on the current traffic situation in the NAT airspace. The reduction of the oceanic separation standards makes it possible for aircraft to perform re-routings within the OTS, and therefore to follow improved trajectories. As a consequence, the total trajectory length and the congestion level in the pre-oceanic airspace significantly decreases.

Another observation that can be made from Table 5 concerns the total number of allowed time slots N_d among which the aircraft track entry delay can be chosen. The fewer the number of allowed slots, N_d, is, the smaller the number of delayed aircraft and total entry delay are: decreasing N_d from 6 to 1 for tests with $F^{(1)}_{obj}$ leads to a significant increase in the number of not-delayed flights from 14% to 50% and to a large decrease of the total entry delay from 80-100 hours to 14 hours. At the same time, it results in an increase of the number of aircraft deviated from their desired entry/exit track (approximately, from 10% to 20%): having lost degrees of freedom for one optimization parameter ($\delta^f \in \{1, ..., N_d\}$), the mutation operator is more often applied to other optimization parameters (TA^f_{in}, TA^f_{out}).

This last observation shows that the two criteria - the number of deviations and the value of delays - are opposite. Thus, the best solutions must

be trade-offs. For the tests with objective function $F_{obj}^{(2)}$, this kind of solution is produced: the number of deviations and the value of delays are minimized simultaneously. As seen from Table 5, such compromise solutions are better than those produced with $F_{obj}^{(1)}$, although they demand more CPU time.

5.3 Simulations with RSS: total cruising time

In this section we concentrate on minimizing the total cruising time, P, as the cruising time is directly related with the fuel consumption, which is the major criterion for airlines. We also take into account the criterion of maximizing the number of attributed desired tracks, as it has a strong influence on the air-traffic congestion. Several simulations with different parameter values are performed in this study. The weighting coefficients are set to: $\alpha = 0$, $\gamma = 1$, $\beta = 1, 0.5, 0.2$ (for Tests 1, 2 and 3 respectively), and we minimize:

- $F_{obj}^{(3)} = C_t + \phi(\beta G + P)$

Some results are presented in Table 6, where the best values are emphasized in **bold**. The number of delay slots, N_d, for these tests is set to 4, since greater freedom in choosing the track-entry time imposes less constraints on the choice of the flight route, which permits, in turn, more flights to follow their optimal routes. Furthermore, the tests are performed with the number of generations N_G equal to 3000. Empirical tests show that increasing N_G from 1000 to 3000 significantly improves the quality of final solutions, while further increasing N_G from 3000 to 5000 only has a marginal effect. The average CPU time of one GA execution for 3000 generations is about 15 minutes.

Table 6 shows that Test 1 ($\beta = 1$) gives the best results in satisfying the desired entry/exit tracks, Test 2 ($\beta = 0.2$) yields the best results in minimizing the cruising times, and the results of Test 3 ($\beta = 0.5$) yield to compromise solutions. Thus, any of these solutions could be satisfying, depending on the priorities of the user.

The presented results show that the choice of entry/exit tracks has a significant impact on the total cruising time. Indeed, when an aircraft is assigned a neighboring track instead of its desired exit (entry) track, this neighboring track is closer to the entry (exit) track, and the aircraft is to perform fewer re-routings within the OTS. Consequently, its route in the OTS will be shorter, and the cruising time will thereby be decreased.

Table 6: Comparison of cruising times and number of attributed desired tracks in simulations with different contributions in the objective function

Test	1	2	3
Weighting coefficient β	1	0.5	0.2
August 3rd			
% of flights with desired entry tracks	**96,4%**	95,5%	63,1%
% of flights with desired exit tracks	**96,7%**	42,6%	19,9%
Total cruising time P (hours)	1050,30	1027,69	**1019,92**
Average cruising time (hours)	3,17	3,10	**3,08**
August 4th			
% of flights with desired entry tracks	**96,3%**	96,0%	59,5%
% of flights with desired exit tracks	**95,2%**	38,4%	27,8%
Total cruising time P (hours)	1176,40	1146,73	**1139,27**
Average cruising time (hours)	3,11	3,03	**3,01**

Another factor that can lead to cruising-time minimization is the choice of wind-optimal tracks. The next section is devoted to the study of the impact of wind on cruising time.

5.4 Impact of the wind on the total cruising time

The wind speed differs from one track to another (see Fig. 8) and from one flight level to another. As in our simulations the FLs are imposed to flights, the gain in cruising time may only be obtained by choosing better WPs to perform the re-routing. Let us further concentrate on the comparison of the obtained cruising times with those provided by the initial FPLs.

The cruising time clearly depends on the aircraft trajectories. Let L^f denote the length of the trajectory along the OTS for flight f. It is computed by summing the lengths of the links (the route segments between the OTS WPs) followed by the aircraft. A decrease of trajectory length means that the trajectory obtained by the optimization algorithm is shorter than the initial FPL trajectory. The value of the length decrease is the difference between the initial (FPL) trajectory length and the resulting (optimized) trajectory length. The cruising-time decrease is defined in an analogous manner, as well as the trajectory-length and cruising-time increases. Table 7 presents some results of comparison, corresponding to Tests 2 and 3 described in the

previous section (note that a negative decrease represents in fact an increase).

Table 7: Comparison of aircraft trajectory length and cruising time for initial FPLs with optimized solutions

Test (Weighting coef. β)		Test 2 ($\beta = 0.5$)		Test 3 ($\beta = 0.2$)	
Value (V)		L^f, (km)	p^f, (hours)	L^f, (km)	p^f, (hours)
August 3rd					
Flights with V	decreased	26,0%	48,3%	44,4%	61,0%
	not increased	29,0%	51,1%	47,7%	64,0%
Average val. of V	decrease	34,68	0,04	39,86	0,04
	increase	62,40	0,06	47,18	0,04
Result val. of V decrease		-11680	-3,90	-2303	3,86
August 4th					
Flights with V	decreased	29,9%	41,8%	41,8%	51,6%
	not increased	31,5%	43,4%	45,0%	54,8%
Average val. of V	decrease	43,42	0,05	46,26	0,05
	increase	55,12	0,06	34,16	0,04
Result val. of V decrease		-9371	-3,24	205	4,22

Test 2 yields solutions for which both the total value of trajectory lengths and the total value of cruising time are increased, although there is a significant number of flights for which these values are decreased. The increase of trajectory length for most flights is not surprising: the trajectories from the FPLs follow in most cases one predefined track, while the trajectories computed by the optimization algorithm include re-routing to satisfy the optimal entry and exit points. The cruising time increase is directly related to the trajectory length increase. However, the number of flights for which p^f is decreased is greater than the number of flights for which L^f is decreased. Thus, there are necessarily some flights that cross the ocean faster, even though they follow longer trajectories. This is certainly due to the use of route segments involving preferable winds. This observation is also confirmed by the results of Test 3, where the cruising time is decreased for more than 50% of all flights. For August 3rd, it is even more evident, as the total value of cruising times is decreased by several hours, while the total value of trajectory lengths is increased.

Another confirmation of this conclusion can be seen from Table 8 that dis-

plays the relationship between cruising-time decrease and trajectory-length decrease. One observes that for about 20% of flights, the decrease of cruising time is clearly obtained due to the selection of wind-optimal routes.

Table 8: Relationship between cruising-time decrease and trajectory-length decrease

	August 3rd, 2006		August 4th, 2006	
	Test 2	Test 3	Test 2	Test 3
% of flights for which:				
p^f is decreased	48,3%	61,0%	41,8%	51,6%
L^f is decreased	25,0%	44,4%	29,9%	41,8%
p^f and L^f are decreased	24,2%	39,3%	23,3%	32,8%
only p^f is decreased	24,2%	21,8%	18,5%	18,8%
only L^f is decreased	1,8%	5,1%	6,6%	9,0%

6 Conclusion

In this paper, a new mathematical model for oceanic air traffic is introduced. Based on the future performances promising the reduction of the current separation standards, a Genetic Algorithm, has been implemented in order to improve aircraft routes and to reduce the induced congestion at the entry/exit continental airspace. Several performance optimization criteria have been implemented, including aircraft departure and destination requirements and cruising time minimization. The influence of the oceanic wind has also been taken into account in simulations. The developed approach has been applied to real North Atlantic airspace traffic data.

The performed simulations show that implementing new technologies will yield a strong positive effect on the traffic in North Atlantic oceanic airspace. The reduction of the current separation standards makes it possible for aircraft to perform re-routing within the Organized Track System, and therefore to follow more optimal trajectories towards their destination. As a consequence, the total flight duration and the congestion level in the pre-oceanic airspace can significantly decrease.

In perspective we intend to treat the presented problem using multi-objective methods. We are also working on a wind networking approach permitting the aircraft en route to receive in real time the information about

the observed winds from preceding aircraft on the same route, that tends to increase the precision in flight prediction. At last, we consider replacing a discrete optimization model with a continuous one, i.e. replacing the predefined discrete tracks with wind-optimal routes for flights crossing the North Atlantic oceanic airspace.

Acknowledgements

This work has been supported by French National Research Agency (ANR) through COSINUS program (project ID4CS nANR-09-COSI-005). The authors wish to thank Marine Feron for proofreading this paper. The authors are very grateful to the anonymous referees for their careful reading and various suggestions that improved significantly the quality of this paper.

References

[1] *NAT Doc 007, Guidance concerning air navigation in and above the North Atlantic MNPS airspace*, 2012th ed., International Civil Aviation Organisation, 2012, published on behalf of the North Atlantic Systems Planning Group (NAT SPG) by the European and North Atlantic Office of ICAO.

[2] *Doc4444, Air Traffic Management*, 15th ed., International Civil Aviation Organisation, 2007.

[3] P. Louyot, "ASEP-ITM simulations from traffic data," DSNA, ASSTAR WP8, Tech. Rep., Sep. 2007.

[4] FAA, "http://www.faa.gov/nextgen/implementation/programs/adsb/," 2012.

[5] M.Prandini, L.Piroddi, S.Puechmorel, and S.L.Brazdilova, "Toward air traffic complexity assessment in new generation air traffic management systems," *IEEE Transactions on Intelligent Transportation Systems*, vol. 12, no. 3, pp. 809–818, Sep. 2011.

[6] P. Massoglia, M. Pozesky, and G. Germana, "The use of satellite technology for oceanic air traffic control," *Proceedings of the IEEE*, vol. 77, no. 11, Nov. 1989.

[7] A. Williams, "Benefits assessment of reduced separations in North Atlantic Organized Track System," CSSI Inc., Advanced Programs, 400 Virginia Ave. SW, Washington, DC, Tech. Rep., 2005.

[8] S. Mohleji and J. Hoffman, "Performance analysis of North Pacific operations using an automated air traffic control system simulation," *IEEE Transactions on Control Systems Technology*, vol. 1, no. 3, pp. 179–185, Sep. 1993.

[9] S. Grabbe, B. Sridhar, and N. Cheng, "Central East Pacific flight routing," in *AIAA Guidance, Navigation, and Control Conference and Exhibition*, Keystone, Colorado, Aug. 2006.

[10] S. Grabbe, B. Sridhar, and A. Mukherjee, "Central East Pacific flight scheduling," in *AIAA Guidance, Navigation, and Control Conference and Exhibition*, Hilton Head, South Carolina, Aug. 2007.

[11] S. Grabbe, B. Sridhar, and A. Mukherje, "Scheduling wind-optimal Central East Pacific flights," *Air Traffic Control Quarterly*, vol. 16, no. 3, pp. 187–210, 2008.

[12] O. Rodionova, M. Sbihi, D. Delahaye, and M. Mongeau, "Optimization of aicraft trajectories in North Atlantic oceanic airspace," in *5th International Conference on Research in Air Transportation - ICRAT 2012*, University of California, Berkeley, California, May 2012.

[13] D. Goldberg, *Genetic Algorithms in Search Optimization and Machine Learning*. Addision Wesley, 1989.

[14] J. Koza, *Genetic Programming*. MIT press, 1992.

[15] O. Rodionova, "http://www.recherche.enac.fr/~mongeau/NATdata.zip," 2013.